JOURNAL OF GUIDANCE, CONTROL, AND DYNAMICS
Vol. 18, No. 3, May–June 1995

# Assumed Modes Method and Articulated Flexible Multibody Dynamics

S. S. K. Tadikonda,* T. G. Mordfin,† and T. G. Hu‡
*Grumman Space Station Integration Division, Reston, Virginia 22090*

**The use of assumed modes in articulated flexible multibody dynamics algorithms requires the evaluation of several domain-dependent integrals that are affected by the type of modes used. The implications of these integrals—often called zeroth-, first-, and second-order terms—are investigated in this paper for arbitrarily shaped bodies whose modal models may be obtained using finite element analyses. Guidelines are developed for using appropriate boundary conditions when generating the component modal models. It is shown that the issue of which body reference frame to use is intimately related to the question of what type of component body modal models must be selected. The issues of whether and which higher order terms must be retained are also addressed. Analytical results, and numerical results using the Shuttle Remote Manipulator System as the multibody system, are presented to qualitatively and quantitatively address these issues.**

## I. Introduction

THE assumed modes method is often employed to model the small elastic deformation in flexible bodies undergoing large overall rigid-body motions.[1–7] The substitution of a modal expansion for the elastic deformation at an arbitrary configuration point on a component body followed by the derivation of the equations of motion results in modal terms that require domain integrations. The integrals consist of modal mass and stiffness terms, rigid-body and elastic motion coupling terms (modal linear and angular momentum coefficients[8]), and higher order terms.[2] The modal integrals, naturally, depend on the type of modes selected. Finite element analyses are required to generate the component body modes for all but uniform beam and plate structures.

A variety of dynamics formulations have been presented in the literature for articulated flexible multibody systems,[1–7] but the question of what type of modes to choose has not been satisfactorily answered. Fixed-free modes,[5,9] pinned-free modes,[1,10] and fixed-mass-augmented modes[11] have all been used in simulations and in controller designs in experiments, to model a flexible link pinned at one end, but no definitive conclusions have been drawn. Experimental investigations of two-link flexible manipulators are also inconclusive.[12] As a result, no generally applicable guidelines are available for specifying geometric boundary conditions (BCs) and outboard body effects in component-body modal representations. Therefore, employing finite element analysis codes such as NASTRAN to model component bodies for use in either generic multibody codes, such as TREETOPS,[2] DISCOS,[3] and GRASP,[7] or problem-specific codes is considered an art rather than a science. The literature is also incomplete on the use of higher order modal terms in numerical simulations. We develop guidelines in this paper for the use of appropriate geometric and natural BCs when generating component modes of a flexible body and specify whether and which higher order modal terms must be retained in articulated multibody dynamics simulations. These recommendations, which are based on analyses of dynamic models, are critical for effectively simulating the dynamics of complex articulated multibody systems such as the space station and the Shuttle Remote Manipulator System (SRMS).

Received June 15, 1993; presented as Paper 93-3710 at the AIAA Guidance, Navigation, and Control Conference, Monterey, CA, Aug. 9–11, 1993; revision received June 23, 1994; accepted for publication July 14, 1994. 

*Senior Flight Systems Engineer; currently Senior Principal Engineer, McDonnell Douglas Aerospace, 7404 Executive Place, Seabrook, MD 20706. Member AIAA.

†Senior Structural Dynamics Engineer; currently Senior Dynamics Engineer, Advanced Marine Enterprises, Arlington, VA 22202. Member AIAA.

‡Engineering Specialist; currently Engineering Specialist, Grumman Technical Services, Inc., Houston, TX 77034. Member AIAA.

## II. Dynamics of a Branch Body

The kinematics and dynamics of a branch body are presented in this section. Using the definition in Ref. 2, a branch body is a body in a multibody chain that has bodies outboard of it. The nomenclature in this paper is as follows: underlined characters represent vectors and superscripts on these vectors denote body association. Subscripts $p$ and $q$ denote nodes that are materially fixed, and $c$ corresponds to center of mass. The boldfaced letter $\mathbf{b}$ denotes body reference frame, and its subscripts $j$ and $L(j)$ correspond to body indices; underlined boldfaced characters denote dyadics. Summation indices are $i$ and $k$.

Consider a branch body, body $j$, and its inboard body, denoted by body $L(j)$, shown in Fig. 1. A body reference frame $\boldsymbol{b}_j = [\underline{b}_{j1}\ \underline{b}_{j2}\ \underline{b}_{j3}]^T$, where $T$ denotes the transpose, is attached to body $j$, and the linear elastic deformation of the body is measured in this frame. The vector $\underline{R}_f^j$ locates the origin of $\boldsymbol{b}_j$ with respect to an inertial reference frame. Hinge $j$ connects and permits articulation (translation and rotation) across nodes $q$ on body $j$ and $p$ on body $L(j)$.

### A. Kinematics

The position of a generic elemental mass d$m$ on body $j$ can be described with respect to the inertial frame by the vector $\underline{R}^j$, defined as

$$\underline{R}^j = \underline{R}_f^j + \underline{r}^j + \underline{u}^j(\underline{r}^j,\ t) \tag{1}$$

where $\underline{r}^j$ defines the location of d$m$ on body $j$ with respect to the origin of $\boldsymbol{b}_j$ in the absence of any elastic deformation, and $\underline{u}^j$ defines the translational elastic deformation at that location. From Fig. 1 we can write

$$\underline{R}_f^j = \underline{R}_f^{L(j)} + \underline{r}_p^{L(j)} + \underline{u}_p^{L(j)} + {}^{L(j)}\underline{y}^j - \left(\underline{r}_q^j + \underline{u}_q^j\right) \tag{2}$$

in which the relative translation of $q_j$ with respect to $p_{L(j)}$ is defined by ${}^{L(j)}\underline{y}^j$. Let

$$\underline{R}_p^{L(j)} = \underline{R}_f^{L(j)} + \underline{r}_p^{L(j)} + \underline{u}_p^{L(j)} \tag{3}$$

Substitution of Eqs. (2) and (3) into Eq. (1) followed by differentiation of Eq. (1) with respect to time in the inertial frame yields the velocity expression

$$\dot{\underline{R}}^j = \dot{\underline{R}}_p^{L(j)} + \underline{\omega}_p^{L(j)} \times {}^{L(j)}\underline{y}^j + \frac{\partial}{\partial t}\left[{}^{L(j)}\underline{y}^j + \underline{u}^j - \underline{u}_q^j\right] + \underline{\omega}^j \times \left(\underline{r}^j + \underline{u}^j - \underline{r}_q^j - \underline{u}_q^j\right) \tag{4}$$

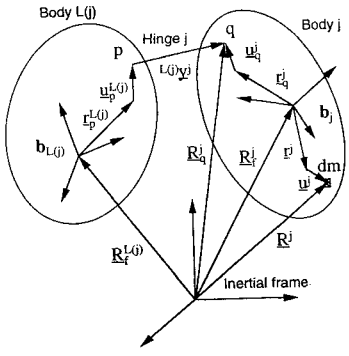


**Fig. 1 Recursive kinematics and generic hinge description.**

A solid dot over a variable denotes differentiation with respect to time in the inertial frame and $\partial/\partial t$ represents differentiation with respect to time in the respective local frames. The angular velocity of body $j$ is denoted by $\underline{\omega}^j$ and that of a reference frame located at the $p$ node on body $L(j)$ is indicated by $\underline{\omega}_p^{L(j)}$, where

$$\underline{\omega}_p^{L(j)} = \underline{\omega}^{L(j)} + \frac{\partial}{\partial t}\left[\underline{u}_p'^{L(j)}\right] \tag{5}$$

and

$$\underline{\omega}^j = \underline{\omega}_p^{L(j)} + {}^{L(j)}\underline{\omega}^j - \frac{\partial}{\partial t}\left(\underline{u}_q'^j\right) \tag{6}$$

Primed variables in the preceding equations denote small rotations due to elastic deformations. The rigid-body angular velocity across hinge $j$ is denoted by ${}^{L(j)}\underline{\omega}^j$. Using a selected Euler sequence to represent these rotations, ${}^{L(j)}\underline{\omega}^j$ can be written as

$${}^{L(j)}\underline{\omega}^j = \sum_{i=1}^{NR_j} \underline{\ell}_i^j \dot{\theta}_i^j \tag{7}$$

The number of rotational degrees of freedom (DOFs) across joint $j$ is denoted by $NR_j$. The unit vectors $\underline{\ell}_i^j$ correspond to the axes of rotation for the selected Euler sequence and defined in the body frame $\boldsymbol{b}_j$, and $\dot{\theta}_i^j (i = 1, \ldots, NR_j)$ are the Euler angle rates.

Similarly, the relative translational velocity across the hinge denoted as $(\partial/\partial t)({}^{L(j)}\underline{y}^j)$ in Eq. (4) can be written in terms of the number of translational DOFs $NT_j$ as

$$\frac{\partial}{\partial t}{}^{L(j)}\underline{y}^j = \sum_{i=1}^{NT_j} \underline{g}_i^{L(j)} \dot{y}_i^j \tag{8}$$

where $\underline{g}_i^{L(j)}$ are the unit vectors defined in the nodal reference frame at the $p$ node on body $L(j)$ along the translational DOFs, and $\dot{y}_i^j (i = 1, \ldots, NT_j)$ denote the associated translational rates.

The elastic deformation for any point on the body can be expressed using a set of assumed modes $\underline{\phi}_i^j$ and their time-dependent amplitudes $\eta_i^j(t)$, with $NM_j$ denoting the number of modes retained in the modal expansion, as

$$\underline{u}^j(\underline{r}^j, t) = \sum_{i=1}^{NM_j} \underline{\phi}_i^j(\underline{r}^j)\eta_i^j(t) \tag{9}$$

Differentiation of Eq. (9) with respect to time in the body frame yields

$$\frac{\partial}{\partial t}\underline{u}^j(\underline{r}^j, t) = \sum_{i=1}^{NM_j} \underline{\phi}_i^j(\underline{r}^j)\dot{\eta}_i^j(t) \tag{10}$$

Note that no restrictions have been placed on the selection of a body frame. Equations (2–6) provide only recursive kinematic relationships between adjacent body frames. We will show in Sec. III. A that the questions of which reference frame and what type of component body modes must be used have the same answer.

### B. Kinetic Energy and Modal Integrals

The kinetic energy for body $j$ is given by

$$KE^j = \frac{1}{2}\int \dot{\underline{R}}^j \cdot \dot{\underline{R}}^j \, dm \tag{11}$$

Let $m^j$ be the mass of body $j$, and $\underline{\boldsymbol{I}}_q^j$ denote the body inertia dyadic about node $q$ on body $j$ defined as

$$\underline{\boldsymbol{I}}_q^j = \underline{\boldsymbol{I}}_{qR}^j + \sum_{i=1}^{NM_j}\left(\underline{\boldsymbol{M}}_i^j + \underline{\boldsymbol{N}}_i^j\right)\eta_i^j + \sum_{i=1}^{NM_j}\sum_{k=1}^{NM_j}\underline{\boldsymbol{P}}_{ik}^j \eta_i^j \eta_k^j \tag{12}$$

where

$$\underline{\boldsymbol{I}}_{qR}^j = \int \left[(\underline{r}^j - \underline{r}_q^j)\cdot(\underline{r}^j - \underline{r}_q^j)\underline{\boldsymbol{U}} - (\underline{r}^j - \underline{r}_q^j)(\underline{r}^j - \underline{r}_q^j)\right] dm \tag{13}$$

$$\underline{\boldsymbol{M}}_i^j = \int \left\{(\underline{r}^j - \underline{r}_q^j)\cdot\left[\underline{\phi}_i^j(\underline{r}^j) - \underline{\phi}_i^j(\underline{r}_q^j)\right]\underline{\boldsymbol{U}} - (\underline{r}^j - \underline{r}_q^j)\left[\underline{\phi}_i^j(\underline{r}^j) - \underline{\phi}_i^j(\underline{r}_q^j)\right]\right\} dm \tag{14}$$

$$\underline{\boldsymbol{N}}_i^j = \left(\underline{\boldsymbol{M}}_i^j\right)^T \tag{15}$$

$$\underline{\boldsymbol{P}}_{ik}^j = \int \left[\underline{\phi}_i^j(\underline{r}^j) - \underline{\phi}_i^j(\underline{r}_q^j)\right]\cdot\left[\underline{\phi}_k^j(\underline{r}^j) - \underline{\phi}_k^j(\underline{r}_q^j)\right]\underline{\boldsymbol{U}}\, dm - \int \left[\underline{\phi}_i^j(\underline{r}^j) - \underline{\phi}_i^j(\underline{r}_q^j)\right]\left[\underline{\phi}_k^j(\underline{r}^j) - \underline{\phi}_k^j(\underline{r}_q^j)\right] dm \tag{16}$$

The unit dyadic is defined by $\underline{\boldsymbol{U}}$ in the preceding equations. The term $\underline{\boldsymbol{I}}_{qR}^j$ represents the rigid-body inertia dyadic about the $q$ node and is denoted as a zeroth-order term because it contains no modal coordinates. Similarly, $\underline{\boldsymbol{M}}_i^j$ and $\underline{\boldsymbol{N}}_i^j$ are denoted as first-order terms and $\underline{\boldsymbol{P}}_{ik}^j$ are denoted as second-order terms, corresponding to the powers of $\eta$ in their coefficients in the inertia dyadic.

In addition to the aforementioned, we define the following modal integrals:

$$\mu_{ik}^j = \int \left[\underline{\phi}_i^j(\underline{r}^j) - \underline{\phi}_i^j(\underline{r}_q^j)\right]\cdot\left[\underline{\phi}_k^j(\underline{r}^j) - \underline{\phi}_k^j(\underline{r}_q^j)\right] dm \tag{17}$$

$$\underline{r}_{qc}^j = \int (\underline{r}^j - \underline{r}_q^j)\frac{dm}{m^j} \tag{18}$$

$$\underline{\alpha}_i^j = \int \left[\underline{\phi}_i^j(\underline{r}^j) - \underline{\phi}_i^j(\underline{r}_q^j)\right] dm \tag{19}$$

$$\underline{h}_i^j = \int (\underline{r}^j - \underline{r}_q^j) \times \left[\underline{\phi}_i^j(\underline{r}^j) - \underline{\phi}_i^j(\underline{r}_q^j)\right] dm \tag{20}$$

$$\underline{Y}_{ik}^j = \int \left[\underline{\phi}_i^j(\underline{r}^j) - \underline{\phi}_i^j(\underline{r}_q^j)\right] \times \left[\underline{\phi}_k^j(\underline{r}^j) - \underline{\phi}_k^j(\underline{r}_q^j)\right] dm \tag{21}$$

The elements of the modal mass matrix are denoted by $\mu_{ik}^j$. The vector $\underline{r}_{qc}^j$ locates the rigid-body center of mass with respect to the $q$ node on body $j$. The terms $\underline{\alpha}_i^j$ and $\underline{h}_i^j$ are known as the modal linear and angular momentum coefficients, respectively. Using the preceding integrals, the kinetic energy of body $j$ given in Eq. (11) can now be expanded as

$$\begin{aligned} KE^j = {} & \tfrac{1}{2}m^j \dot{\underline{R}}_q^j \cdot \dot{\underline{R}}_q^j + \tfrac{1}{2}\underline{\omega}^j \cdot \underline{\boldsymbol{I}}_q^j \cdot \underline{\omega}^j \\ & + \frac{1}{2}\sum_{i=1}^{NM_j}\sum_{k=1}^{NM_j}\mu_{ik}^j \dot{\eta}_i^j \dot{\eta}_k^j + \dot{\underline{R}}_q^j \cdot \sum_{i=1}^{NM_j}\underline{\alpha}_i^j \dot{\eta}_i^j \\ & + \dot{\underline{R}}_q^j \cdot \left[\underline{\omega}^j \times \left(m^j \underline{r}_{qc}^j + \sum_{i=1}^{NM_j}\underline{\alpha}_i^j \eta_i^j\right)\right] \\ & + \underline{\omega}^j \cdot \left[\sum_{i=1}^{NM_j}\underline{h}_i^j \dot{\eta}_i^j + \sum_{i=1}^{NM_j}\sum_{k=1}^{NM_j}\underline{Y}_{ik}^j \eta_i^j \dot{\eta}_k^j\right] \end{aligned} \tag{22}$$

in which

$$\underline{\dot{R}}_q^j = \underline{\dot{R}}_p^{L(j)} + \underline{\omega}_p^{L(j)} \times {}^{L(j)}\underline{y}^j + \frac{\partial}{\partial t}\left[{}^{L(j)}\underline{y}^j\right] \tag{23}$$

Inspection of the terms in the kinetic energy expression along with a Lagrangian formulation of the equations of motion reveals that $\underline{\alpha}_i^j$ and $\underline{h}_i^j$ are zeroth-order terms, $\underline{Y}_{ik}^j$, $\underline{M}_i^j$, and $\underline{N}_i^j$ are first-order terms, and $\underline{P}_{ik}^j$ is a second-order term. The relevance and significance of these terms will be discussed in Sec. III.

### C. Modal Coupling Terms

Modal coupling terms represent the coupling between the rigid body and elastic motions and can be derived using the kinematic relationships presented in Sec. II.A. (Reference 2 presents the general procedure.) We first consider the translational-modal coupling terms. For $\xi$ corresponding to the equation of motion (EOM) associated with the $i$th translational DOF at joint $j$, and $\zeta$ corresponding to the $k$th modal DOF of body $j$, these can be shown to be

$$M_{\xi\zeta} = \underline{g}_i^{L(j)} \cdot \left( \underline{\alpha}_k^j + \sum_n \sum_{s=1}^{a_n} {}^j m^{ns} \times \left\{ \underline{\phi}_k^j\left(\underline{r}_{pn}^j\right) - \underline{\phi}_k^j\left(\underline{r}_q^j\right) + \left(\underline{r}_{pn}^j - \underline{r}_q^j\right) \times \underline{\phi}_k'^j\left(\underline{r}_q^j\right) + \left[\underline{\phi}_k'^j\left(\underline{r}_{pn}^j\right) - \underline{\phi}_k'^j\left(\underline{r}_q^j\right)\right] \times \left(\underline{Z}^{js} + \underline{r}_{qc}^s\right) \right\} \right) \tag{24}$$

where

$$\underline{Z}^{js} = \underline{X}^{js} - \left(\underline{r}_{pn}^j + \underline{u}_{pn}^j\right) + \left(\underline{r}_q^j + \underline{u}_q^j\right) \tag{25}$$

and $\underline{X}^{js}$ is the vector from node $q$ on body $j$ to node $q$ on body $s$. The summation in Eqs. (24) and (25) is carried over body $j$ and all bodies $s$ outboard of it. Since a generic branch body can lead to more than one outboard branch, we introduce the summation index $n$ to identify the branch that is outboard of body $j$. Thus, $n$ has a maximum value corresponding to the number of branches that are outboard of body $j$, and $a_n$ corresponds to the total number of bodies in the $n$th branch outboard of body $j$. The mass of the $s$th body in the $n$th branch outboard of Body $j$ is denoted by ${}^j m^{ns}$ in the preceding equation.

Next, we consider the rotational-modal coupling terms. These can be shown to be

$$M_{\xi\zeta} = \underline{\ell}_i^j \cdot \left( \underline{h}_k^j + \sum_n \sum_{s=1}^{a_n} \left(\underline{X}^{js} + \underline{r}_{qc}^s\right) \times {}^j m^{ns} \left\{ \underline{\phi}_k^j\left(\underline{r}_{pn}^j\right) - \underline{\phi}_k^j\left(\underline{r}_q^j\right) + \left(\underline{r}_{pn}^j - \underline{r}_q^j\right) \times \underline{\phi}_k'^j\left(\underline{r}_q^j\right) + \left[\underline{\phi}_k'^j\left(\underline{r}_{pn}^j\right) - \underline{\phi}_k'^j\left(\underline{r}_q^j\right)\right] \times \underline{Z}^{js} \right\} + \sum_n \sum_{s=1}^{a_n} {}^j m^{ns} \underline{X}^{js} \times \left\{ \left[\underline{\phi}_k'^j\left(\underline{r}_{pn}^j\right) - \underline{\phi}_k'^j\left(\underline{r}_q^j\right)\right] \times \underline{r}_{qc}^s \right\} + {}^j\underline{I}_q^{ns} \cdot \left[\underline{\phi}_k'^j\left(\underline{r}_{pn}^j\right) - \underline{\phi}_k'^j\left(\underline{r}_q^j\right)\right] \right) \tag{26}$$

The subscript $\xi$ now corresponds to the EOM associated with the $i$th rotational DOF at joint $j$, and $\zeta$ corresponds to the $k$th modal DOF of body $j$. The variable ${}^j\underline{I}_q^{ns}$ represents the inertia dyadic of body $s$ that is in the $n$th branch outboard of body $j$ about the $q$ node on body $s$. All of the terms in Eqs. (24–26) contain flexibility contributions either directly or through rotational transformations.

## III. Significance of Zeroth-Order Modal Integrals

Among the various modal integrals presented in Sec. II.B, the zeroth-order terms are the most important ones in the synthesis of flexible multibody dynamics equations. This is because they determine the characteristics of the linearized system. The expressions given in Sec. II.C for the elements of the system mass matrix facilitate the kind of analysis needed to answer questions about selecting the most appropriate reference frames and type of modes. In this section, we investigate joint articulation and outboard body effects and point out the need for consistency between generating component flexibility models and using such models in a multibody dynamics environment.

### A. Joint Articulation Effects

Joint articulation effects depend on the consistency between the geometric boundary conditions present in the multibody system and those used to generate the component flexible body model. To illustrate, consider a flexible leaf body (one that does not have any outboard bodies) in a tree topology that is free to translate along the $i$th translational DOF at hinge $j$. If the component modes are obtained by imposing this BC at node $q$ on body $j$, then the expression in Eq. (24) vanishes, i.e.,

$$M_{\xi\zeta} = \underline{g}_i^{L(j)} \cdot \underline{\alpha}_k^j = 0 \tag{27}$$

Similarly, if this body is free to rotate about an axis $\underline{\ell}_i^j$-at node $q_j$, and the body $j$ component modes satisfy this BC, then the modal coupling term in Eq. (26) vanishes:

$$M_{\xi\zeta} = \underline{\ell}_i^j \cdot \underline{h}_k^j = 0 \tag{28}$$

Equations (27) and (28) represent the orthogonality of the rigid-body translational and rotational modes to the flexible modes.

However, if the geometric BCs used in the multibody model are different from those imposed when the component modes are generated, Eqs. (27) and (28) no longer hold. The theoretical as well as practical implications of such a scenario will be investigated in the following example.

*Example 1:* A uniform beam, flexible in the $\underline{b}_{11}\underline{b}_{12}$ plane and free to rotate about the $\underline{b}_{13}$ axis, is shown in Fig. 2. Let $\rho$ be the mass per unit length of the beam, $\sigma$ the beam length, and $EI$ the beam stiffness. The spatial coordinate $x$ is measured from the pinned end along the underformed beam axis, the unit vector along which is denoted by $\underline{b}_{11}$. If we use mass-normalized cantilever modes $\psi_i$ (eigenvalues $\lambda_i$) to represent the elastic deflection of the beam due to bending, i.e., $\underline{\phi}_i = \psi_i \underline{b}_{12}$, where

$$\psi_i = \frac{1}{\sqrt{\rho\sigma}}\left[\cosh\beta_i x - \cos\beta_i x + A_i(\sin\beta_i x - \sinh\beta_i x)\right] \tag{29}$$

$$A_i = (\sinh\lambda_i - \sin\lambda_i)/(\cos\lambda_i + \cosh\lambda_i) \tag{30}$$

and $\beta_i = \lambda_i/\sigma$, it can be shown that

$$\underline{\ell}_1^1 \cdot \underline{h}_i^1 = \underline{b}_{13} \cdot \underline{h}_i^1 = H_i = 2\sigma\sqrt{\rho\sigma}\Big/\left(\lambda_i^2\right) \tag{31}$$

Let $H = [H_1\ H_2\ \ldots\ H_{NM1}]$ and $\eta = [\eta_1\ \eta_2\ \ldots\ \eta_{NM1}]^T$. With an applied torque $\tau$ at the pinned end, the linearized equations of motion for this $NM_1 + 1$ DOF system can be shown to be

$$\begin{bmatrix} I_0 & H \\ H^T & [\mu_{ik}] \end{bmatrix} \begin{Bmatrix} \ddot{\theta} \\ \ddot{\eta} \end{Bmatrix} + \begin{bmatrix} 0 & 0 \\ 0 & [\omega_i^2] \end{bmatrix} \begin{Bmatrix} \theta \\ \eta \end{Bmatrix} = \begin{Bmatrix} 1 \\ \left[\left(\dfrac{d\psi_i}{dx}\right)_{x=0}\right] \end{Bmatrix} \tau = B\tau \tag{32}$$

where $[\mu_{ik}]$ is the $NM_1 \times NM_1$ modal mass matrix, $I_0 = \rho\sigma^3/3$, $[\omega_i^2]$ is a diagonal $NM_1 \times NM_1$ modal stiffness matrix whose $i$th diagonal element $\omega_i^2$ is given by

$$\omega_i^2 = \lambda_i^4 EI/(\rho\sigma^4) \tag{33}$$

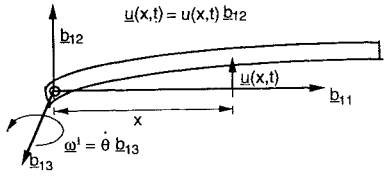


**Fig. 2 Flexible pinned-free link.**

**Table 1 Comparison of eigenvalues**

| Fixed-free eigenvalues | $\gamma$ for the homogeneous system in Eq. (32) for various $NM_1$ | | | | | Pinned-free eigenvalues |
|---|---|---|---|---|---|---|
| | $NM_1 = 1$ | $NM_1 = 2$ | $NM_1 = 3$ | $NM_1 = 4$ | $NM_1 = 5$ | |
| | 0 | 0 | 0 | 0 | 0 | 0 |
| 1.8751 | 4.5321 | 3.9288 | 3.9268 | 3.9267 | 3.9267 | 3.9266 |
| 4.6941 | —— | 8.6082 | 7.0806 | 7.0706 | 7.0694 | 7.0686 |
| 7.8548 | —— | —— | 12.7750 | 10.2359 | 10.2161 | 10.2102 |
| 10.9955 | —— | —— | —— | 16.9904 | 13.3929 | 13.3518 |
| 14.1372 | —— | —— | —— | —— | 21.2565 | 16.4934 |

**Table 2 Comparison of model control influence coefficients**

| | Elements of $\sigma\sqrt{\rho\sigma}\Phi^T B$ (magnitudes for vibrational modes only) | | | | | $\phi_i'(0)$ for pinned-free modes |
|---|---|---|---|---|---|---|
| $i$ | $NM_1 = 1$ | $NM_1 = 2$ | $NM_1 = 3$ | $NM_1 = 4$ | $NM_1 = 5$ | (magnitudes only) |
| 1 | 9.9673 | 5.4024 | 5.4005 | 5.4004 | 5.4004 | 5.4004 |
| 2 | —— | 24.9110 | 9.9712 | 10.0033 | 10.0074 | 10.0085 |
| 3 | —— | —— | 44.1209 | 14.2547 | 14.4031 | 14.4386 |
| 4 | —— | —— | —— | 66.9567 | 18.4274 | 18.8823 |
| 5 | —— | —— | —— | —— | 92.9127 | 23.3251 |

and $(d\psi_i/dx)_{x=0} = 0$ for cantilever modes. Note that because of mass normalization $\mu_{ik} = \delta_{ik}$, where $\delta_{ik}$ represents the Kronecker delta.

We now solve for the frequencies $\Omega_i (i = 1, \ldots, NM_1 + 1)$ of the homogeneous system in Eq. (32) for various numbers of retained flexible modes and define $\gamma_i$ such that $\gamma_i^4 = \Omega_i^2 \rho\sigma^4/EI$. The objectives behind this definition are twofold: one is that since $\gamma_i$ are nondimensional quantities the results from this analysis will be independent of the beam properties and the second is that this form for $\gamma_i$ is similar to that for $\lambda_i$ define in Eq. (33). The results are shown in Table 1. Also shown in Table 1 are the eigenvalues for component cantilever modes and pinned-free modes for a uniform flexible beam. From this table, it is clear that the system in Eq. (32) approximates a component pinned-free beam instead of a component cantilever beam. In addition, the largest value of $\gamma_{NM_1+1}$ is always much higher than that of the corresponding pinned-free mode. The resulting high-frequency $\Omega_{NM_1+1}$ can force the use of an unreasonably small integration time step during a time domain analysis. In addition, although the lowest system frequencies may be obtained to within a desired accuracy limit, the mode shapes will be a different matter. A system frequency response study would indicate this.

From Table 1 we observe that in order to represent the first two "system" flexible modes to a three digit accuracy, we must use at least five component cantilever modes. The use of five cantilever modes, however, causes the generation of a very high frequency system mode. This is because the system frequencies are proportional to the squares of the eigenvalues shown in Table 1. We therefore see two disadvantages to using cantilever component modes: in order to attain a desired accuracy, we unnecessarily both increase the order of the system and make it numerically stiff.

We now look at how the control influence coefficient matrix $B$ in Eq. (32) is transformed when the eigensolution of the corresponding homogeneous system is used to uncouple the equations. Recall that $B$ in Eq. (32) is given by $B = [1\,0\,0 \cdots 0]^T$ when cantilever modes are used. Let the $(NM_1 + 1) \times (NM_1 + 1)$ matrix containing the mass-normalized eigenvectors of the homogeneous system in Eq. (32) be defined by $\Phi$. Substitution of the transformation $[\theta\eta^T]^T = \Phi\nu$, where $\nu$ is a column matrix containing the generalized coordinates, in Eq. (32) and then premultiplication by $\Phi^T$ result in a set of uncoupled (modal) equations. The resulting nondimensionalized modal control influence coefficients (the elements of $\sigma\sqrt{\rho\sigma}\Phi^T B$) are shown in Table 2 for various $NM_1$. Also shown in this table are the slopes of pinned-free modes at the pinned end. Because of the nonuniqueness of the eigenvectors (to a sign), only the magnitudes of these coefficients are shown and compared with those of the pinned-free modes. Convergence as $NM_1$ is increased is apparent for the first mode. Although results for the other coefficients are similar, the convergence for the second and higher modes clearly does not follow the pattern of the eigenvalues, for which the convergence is restricted to be from above.

We also observe from Table 2 that although $B_2 = B_3 = \cdots = B_{NM_1+1} = 0$ for the component cantilever modes, the *system* modal influence coefficients are not zero, and they indeed converge to those of the component pinned-free modes. These are also the characteristics of results when static modes, simple polynomials, or any other set of trial functions that have both a zero displacement and a zero slope at the pinned end are used as the component assumed mode shapes. Using pinned-free modes, however, has the advantage of neither unnecessarily increasing the order of the system, nor making it numerically stiff, while generating the most accurate *system* modes possible.

This example clearly points to the need for consistency between the geometric BCs that are used to generate component-body flexibility models and the geometric BCs present in the articulated multibody system.

Inconsistent modeling of the geometric BCs may also cause mass matrix singularities. This can be easily seen in the context of the one link flexible manipulator considered earlier, by invoking the properties of the cantilever modes given by Hughes.[8] Since the eigenfunctions in Eq. (29) are mass normalized, the product $HH^T$ approaches the rigid-body inertia $I_0$ as $NM_1 \to \infty$. Using Eq. (31) in computing $HH^T$ yields 0.9986* $I_0$ with $NM_1 = 3$ and 0.9994* $I_0$ with $NM_1 = 4$. Thus, as $NM_1$ increases, the condition number of the mass matrix increases, ultimately resulting in ill-conditioning. In the context of the component modes that are generated using the finite element method, the use of all of the cantilever modes in Eq. (32) will yield a singular mass matrix. However, if pinned-free component modes are used to obtain the EOM in Eq. (32), $H_i = 0$ for each of the modes. Then the rigid-body motion equation in Eq. (32) decouples from the modal equations and the numerical problems do not arise. □

We can arrive at this conclusion from still another perspective. We stated in Sec. II. A that no constraints are imposed on the selection of body frames and that these frames are defined only through the kinematic relationships in Eqs. (2–7). From the preceding example, we conclude that the selection of consistent geometric BCs for component mode generation also results in the most appropriate choice for the body reference frame. Specifically, since pinned-free modes have the property that the modal angular momentum coefficient associated with rotation about the pinned axis is identically zero for each of the modes, a body frame with respect to which the pinned-free modes are generated can be recognized as the frame that naturally satisfies the angular momentum constraint associated with the flexible motion. The modal angular momentum constraint is one of the mode shape constraints[13] that can be used to define the body frame. The other is the modal linear momentum constraint. If the translational DOFs are also present and the modal linear momentum

coefficients vanish as well, then the modes are said to satisfy the linearized Tisserand constraint.[13]

The advantage of each mode contributing a zero angular/linear momentum with respect to the body frame is that it provides a straightforward way of working with the rigid-body frame.[13] The elastic deformation is then expressed in terms of the deformational coordinates only. In Example 1, this is precisely what the transformation of Eq. (32) into $\nu$ coordinates using the eigenvector matrix $\Phi$ achieves. The $\nu$ coordinates provide a body frame with respect to which the angular momentum constraint is satisfied, as well as the corresponding flexible motion coordinates.

From the preceding analyses, we conclude that modal model generation using the correct geometric BCs is not an option but is rather necessary for an accurate mathematical representation of the physical system.

### B. Outboard Body Effects

The bodies outboard of a branch body also contribute to the rigid-elastic motion coupling terms, as indicated in Eqs. (24) and (26). The outboard body dynamic effects, manifest in these equations through mass and inertia augmentation, also imply natural boundary conditions at the outboard joints. As a result, the component eigensolution must then consider these augmentation effects. This is illustrated using the following example.

*Example 2:* We revisit the system considered in Example 1 and attach an end mass $M_e$. With the mass-normalized cantilever modes in Eq. (29) as the component trial functions, the rigid and elastic motion coupling term in Eq. (26) can be shown to be

$$(H_i)_{\text{coupled}} = (H_i)_{\text{beam}} + M_e \sigma \psi_i(\sigma) \tag{34}$$

where $(H_i)_{\text{beam}} = H_i$ given in Eq. (31). The rigid-body inertia term becomes $I_0 + M_e\sigma^2$ and the modal mass terms are given by

$$\mu_{ik} = \delta_{ik} + M_e \psi_i(\sigma)\psi_k(\sigma) \tag{35}$$

If pinned-free beam modes are selected as the trial functions, then $(H_i)_{\text{beam}} = 0$, but the rigid-elastic motion coupling still remains, i.e., $(H_i)_{\text{coupled}} \neq 0$. Similarly, the modal mass block remains fully coupled. Thus, neither cantilever nor pinned-free modes provide an accurate system description. However, the use of pinned-mass augmented modes with the mass normalization

$$\mu_{ik} = \int_0^\sigma \rho \psi_i(x)\psi_k(x)\,dx + M_e\psi_i(\sigma)\psi_k(\sigma) = \delta_{ik} \tag{36}$$

yields a diagonal modal mass block and makes $(H_i)_{\text{coupled}}$ vanish. The result is a simple mass matrix, a high-fidelity component model with relatively a small number of assumed modes, and a highest frequency in the system that is the same as the highest frequency in the component model. □

Although this can be achieved when only a single outboard point mass is present the extension to other multibody systems is not as straightforward. This is because, as can be seen from Eqs. (24) and (26), the coupling is configuration dependent. This coupling can be made to vanish for a selected configuration by obtaining the effective mass and inertia of all of the outboard bodies across each of the outboard nodes of a body, during the component modal analysis. Although the mass matrix becomes fully populated as the configuration changes, it can be expected that the condition number of the mass matrix will remain reasonable. One advantage of this approach is that the augmented modes enable the satisfaction of the natural BCs in the multibody synthesis. Another advantage is that mass matrix singularities similar to those that were reported in Ref. 14 (using nonaugmented cantilever modes) can be avoided.

For a branch body, from a structural dynamics perspective, the location of the joint leading to its outboard bodies should not be modeled as dynamically free when generating the component eigensolution. This is because a "free" end implies zero force and moment conditions, and that forces and moments due to outboard bodies cannot be balanced by the body elastic forces at that location. The use of "free" natural boundary conditions at the end leading to outboard bodies when generating the component modes would clearly lead to the violation of the force and moment balance at that end. This becomes evident if one obtains the elastic motion equations for the flexible bodies in the articulated multibody system using a Newton–Euler formulation. It was shown in Ref. 15 that trial functions must be capable of satisfying the natural as well as the geometric boundary conditions to obtain not only convergence but also an accurate model for the physical system. Thus, the present result from an articulated multibody analysis is consistent with the structural dynamics requirement for accommodating natural BCs.[15] In addition, if continuum-based trial functions are used, care must be taken so that the complementary boundary conditions[15] are not violated.

If the outboard body masses and inertias are considered when generating component modes, the modal momentum coefficients discussed in Sec. III. A vanish only for the configuration for which the modes are generated. For any other configuration, the modes thus generated can only be called trial functions. Consequently, the rigid-body frame ceases to be the Tisserand frame.

## IV. Higher Order Terms and Softening and Stiffening Effects

Of the higher order terms defined in Eqs. (14–16) and (21), only the $\underline{\boldsymbol{P}}^j_{ik}$ term in Eq. (16) has received much attention in the literature. In this section, we discuss the significance of all of the higher order terms. We first consider the first-order terms, present a discussion of the second-order terms, and propose guidelines for the use of these terms in multibody dynamics simulations.

### A. First-Order Terms

The first-order terms, namely, $\underline{\boldsymbol{M}}^j_i$, $\underline{\boldsymbol{N}}^j_i$, and $\underline{\boldsymbol{Y}}^j_{ik}$, do not contribute to the dynamics of single flexible links with beam-type structures undergoing planar slews. For example, if the undeformed beam axis is denoted by $\underline{b}_{11}$ and the rigid-body rotational axis is in the $\underline{b}_{12}\underline{b}_{13}$ plane, then due to the transverse nature of the elastic motion of the beam,

$$\underline{\omega}^j \cdot \underline{Y}^j_{ik} = \underline{\omega}^j \cdot \int \underline{\phi}^j_i \times \underline{\phi}^j_k \, dm = 0 \tag{37}$$

and

$$\underline{\omega}^j \cdot \boldsymbol{M}^j_i \cdot \underline{\omega}^j = \underline{\omega}^j \cdot \boldsymbol{N}^j_i \cdot \underline{\omega}^j = 0 \tag{38}$$

Equations (37) and (38) thus explain the absence of these terms from the equations of motion presented in the literature for flexible single link and planar two link manipulators.

Now, consider the following term that appears in the modal equations of body $j$ [using the kinetic energy in Eq. (22) via a Lagrangian formulation]:

$$\tfrac{1}{2}\underline{\omega}^j \cdot \frac{\partial \underline{\boldsymbol{I}}^j_q}{\partial \eta^j_i} \cdot \underline{\omega}^j = \underline{\omega}^j \cdot \left[\tfrac{1}{2}\left(\underline{\boldsymbol{M}}^j_i + \underline{\boldsymbol{N}}^j_i\right)\right] \cdot \underline{\omega}^j + \underline{\omega}^j \cdot \sum_{k=1}^{NM_j} \underline{\boldsymbol{P}}^j_{ik}\eta^j_k \cdot \underline{\omega}^j \tag{39}$$

It can be seen that the first-order terms in the inertia dyadic appear as zeroth-order terms in the body modal equations. The presence of a product involving various $\underline{\omega}^j$ on the left-hand side of Eq. (39) indicates that this is a nonlinear term for nonprescribed motions. Referring to Eq. (14), we see that the conditions for the terms in Eq. (39) to not vanish are 1) $(\underline{r}^j - \underline{r}^j_q) \cdot [\underline{\phi}^j_i(\underline{r}^j) - \underline{\phi}^j_i(\underline{r}^j_q)] \neq 0$ or 2) $\underline{\omega}^j \cdot (\underline{r}^j - \underline{r}^j_q) \neq 0$ and $\underline{\omega}^j \cdot (\underline{u}^j - \underline{u}^j_q) \neq 0$. Note that all of these conditions are not satisfied for single flexible links that undergo planar slews. The issue of whether these terms should be retained for nonplanar systems will be investigated in Sec. V using a numerical example.

### B. Second-Order Terms

The last term in Eq. (39) enters the modal equations for body $j$ as a softening term, if and only if it is not identically equal to zero. This term is nonvanishing in the case of the flexible beam shown in Fig. 2 and considered in Example 1. However, it does vanish in the case of the helicopter blade problem commonly depicted, for example as in Ref. 16 (p. 235).

The deleterious effect of the softening term, along with the remedies, has been the subject of numerous investigations in recent

years.[1,6,14,17–21] Note that not only generic multiflexible body dynamic simulation codes but also hand-derived ad hoc equations of motion contain this softening term. Reference 14 suggests omitting the $\underline{P}^j_{ik}$ term altogether. It was pointed out in Ref. 17 that this recommendation alone is not sufficient for a flexible branch body, and if component modal models do not consider augmentation effects due to outboard bodies, because the outboard bodies also cause softening terms.

### C. Guidelines for Use of Second-Order Terms

The dynamic equations can be used to analyze the effects of 1) prescribed rigid-body motions and 2) prescribed external forces/torques. A spin-up maneuver is a common choice for studying the prescribed rigid-body motion effects in rigid core-flexible appendage systems.[18–21] In doing so, it is assumed that the effect of the appendage vibration on the rigid-body motion of the body to which it is attached is insignificant. This coupling becomes significant if the base and appendage masses are of similar magnitude. Another assumption is that the actuators can provide the forces and torques required to produce desired rigid-body motions. The calculation of the forces and torques that would yield the desired rigid-body motions requires a computer-oriented inverse dynamics approach for all but trivial problems. The engineer or analyst must consider the design and application criteria together for the problem at hand and determine if the required forces or torques for a prescribed motion study are within the actuator limits.

The effects of prescribed forces/torques are often studied for articulated manipulator type rigid or flexible multibody systems where a controller may be present for each articulated degree of freedom. In these systems, each joint will have an actuator and very few joints permit a 360-deg angular motion. For example, the SRMS elbow pitch joint permits only a 162-deg rotation. Repositioning or reorientation maneuvers with these systems do not involve significant softening or significant stiffening due to self-rigid-body motion.[14,17,19] To quote Ryan[19]: "For repositional motions during which bodies do not complete a full revolution, the neglected dynamic stiffness terms tend to be of little consequence. Hence the analysis of spacecraft slewing maneuvers may be performed effectively with [the existing] multibody programs."

If the softening effects are unacceptable (this conclusion can be reached, for the problem at hand, by performing simulations with and without the second-order terms), geometric stiffening effects may be added. For non-beam-type structures that require finite element models, this requires the generation of 21 geometric stiffness matrices to model the stiffening effects due to body self motions.[6] In the case of a branch body, its outboard bodies also contribute to softening as well as stiffening.[17] The link and motor designs for the multibody modeling, verification, and control experiments were used in Ref. 17 to demonstrate that the softening and stiffening effects due to outboard body motions dominate those due to body self motions even for link masses of similar magnitude.

It can be verified that if component modal models are generated using the proper outboard body mass and inertia augmentations as suggested in Sec. III.B, then omitting the second-order terms truly implies omitting all of the softening terms due to both self motions and outboard body motions.[17] Although this is true for all planar manipulator configurations, it is valid only for the selected configuration for nonplanar systems or if the rigid-body maneuvers are not large.

## V. Numerical Results

Two examples are presented using the upper and lower arms of the SRMS, shown in Fig. 3, as the multibody system. The first example demonstrates the effectiveness of the mass and inertia augmented modes, and the second one provides insight into the first-order term effects, discussed in Secs. III.B and IV.A, respectively.

The first example is a three-body problem consisting of the SRMS upper and lower arms in the stretched out configuration connected by a locked joint and a rigid spherical payload of 100 slugs and 100 slug-ft$^2$ rigidly attached at the end of the lower arm. Two component mode sets are used: 1) free-free modes for the upper arm and fixed-free modes for the lower arm, and 2) free-mass and inertia augmented

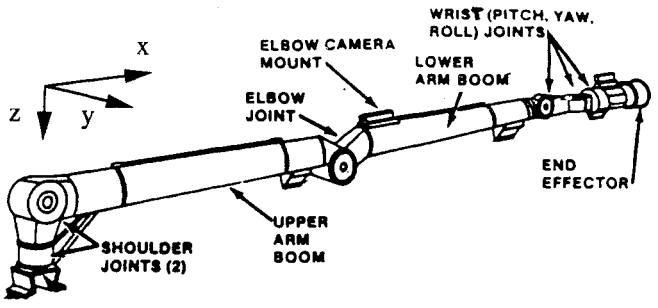


**Fig. 3 Shuttle Remote Manipulator System (SRMS).**

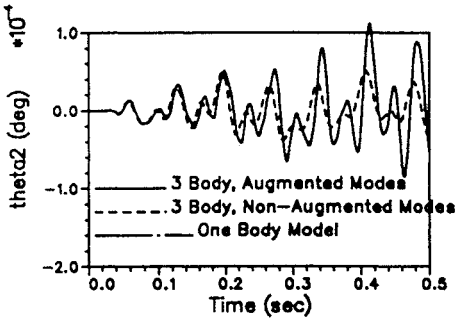


**Fig. 4 Performance of the two mode sets compared with one-body model.**

modes for the upper arm and fixed-mass and inertia augmented modes for the lower arm. All component modes below 1000 Hz are used in the simulations. Although the shoulder joint connects the SRMS to the Shuttle, we consider the SRMS by itself in this study. A one-body free-free model of the entire system is also created for this configuration and serves as the truth model. The multibody system is free both to translate and to rotate with respect to the inertial frame. The component body models are generated using NASTRAN, and the dynamic response in all cases is generated using the articulated multibody dynamics program GRASP.[7] A torque of 5 ft-lb is applied at the upper arm shoulder about the $z$ axis for a period of 0.2 s. This example is motivated by a question that is commonly asked: "If we lock all the joints, can we replicate the response of the single body system using a multibody dynamics (component body) model?"

The dynamic response of the three-body model is compared with that of the one-body model. Figure 4 focuses on the first 0.5 s of the second Euler angle response for all three models. The response of the three-body augmented mode model exactly matches that of the one-body model. However, the response of the three-body nonaugmented model is significantly different. The advantage of accounting for the augmentation effects is thus apparent. Other state responses (not shown) exhibit similar behavior.

We concluded in Sec. III.B from an articulated multibody dynamics perspective as well as a structural dynamics perspective, that outboard body mass and inertia augmentation effects must be considered when generating the branch body component modes, to provide an accurate description of a flexible branch body. The response shown in Fig. 4 for the one-body model demonstrates the effectiveness of mass augmented component models. Note that each of the assumed modes in a component satisfy the same geometric BCs. This is in contrast to other synthesis procedures such as the quasicomparison function approach (Ref. 22) in which it is possible that none of the modes may satisfy the geometric BCs individually. The use of only one set of modes is clearly practical and easy to pursue especially when the component modes for each body must be generated using a finite element code such as NASTRAN for use with a multibody dynamics code such as TREETOPS,[2] DISCOS,[3] or GRASP.[7]

The second example involves the aforementioned three-body model attached at the shoulder to a 200 slug, 200 slug-ft$^2$ rigid, spherical base body. The base body has three rotational and no translational DOFs with respect to the inertial space. A pitch DOF exists between the base body and the upper arm and between the upper and the lower arms. The shoulder (elbow) joint axis corresponds to

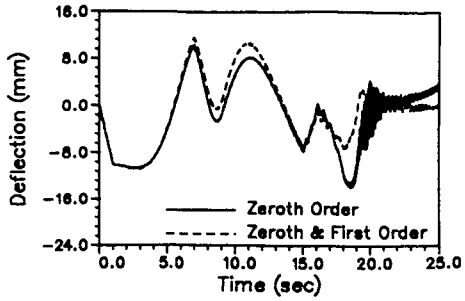


**Fig. 5 Upper arm $y$ deflection with zeroth- and first-order terms; large applied torques.**

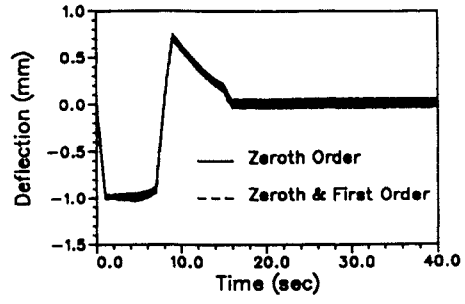


**Fig. 6 Upper arm $y$ deflection with zeroth- and first-order terms; small applied torques.**

the body $y$ axis for the upper (lower) arm. The initial angle at the elbow is 135 deg. Open-loop torques are applied across the SRMS joints and the three axes of the base body. The $y$ deflection of the upper arm at the elbow is shown as a representative result in Fig. 5. The plot shows the result with and without the first-order terms. The effect of including these terms is apparent. Although the applied torques at the SRMS joints are within the actuator limits, the base body undergoes about 1000 deg rotation and the elbow pitch joint rotates about 600 deg during the simulation. Note that these rotations are kinematically not possible for the SRMS. The results from a more reasonable maneuver, in which the large rigid-body rotations are limited to about 120 deg, are shown in Fig. 6, and the first-order terms have no significant effect.

## VI. Conclusions

A variety of flexible multibody dynamics formulations have been presented in the past using the assumed modes method, but, to the best of the authors' knowledge, no general guidelines are available for the users of software tools that are based on such formulations. The analyses presented here for the zeroth-, first-, and second-order modal integrals that arise in these formulations provide guidance for selecting component modes and for retaining higher order terms.

On the basis of these analyses we propose the following guidelines for the users of multi-flexible-body dynamics simulation codes: 1) selecting geometric boundary conditions in the component flexible body models that are consistent with those in the multibody dynamics model, 2) modeling outboard body mass and inertia augmentation effects when generating the component body models, and 3) using the first-order modal integrals only when components undergoing nonplanar rigid-body rotations have nonplanar modes and when the rotational rates are considerably large. We demonstrated that the issue of the choice of a body reference frame is linked to the type of component modes used, which, in turn, is related to the first recommendation.

Regarding the second-order terms, we recalled that softening effects do not arise in helicopter blade problems, although a multibody formulation without the geometric nonlinear terms cannot predict blade stiffening. Appropriately modeled flexible manipulator systems undergoing repositional maneuvers may not be affected by the softening terms in modal equations. We pointed out that prescribed motion studies, when conducted, must meet the design and application criteria for any specific multibody system and must consider actuator and kinematic limits. We believe that the guidelines presented here enable the engineer/analyst to make appropriate judgments regarding the stiffening terms. The Shuttle Remote Manipulator System used in numerical simulations provided the required complexity to authenticate the modeling issues that were addressed in the theoretical parts of this paper.

## Acknowledgments

This paper is based on work performed for the NASA Space Station Freedom Program Office under Contract NASW-4300. We thank Jalal Mapar, Manager, Integrated Systems Performance, for his support and Tom Lewis for his help with the plot package. We also thank an anonymous reviewer for pointing out that the issue of body reference frames must be considered for completeness.

## References

[1]Baruh, H., and Tadikonda, S. S. K., "Issues in the Dynamics and Control of Flexible Robot Manipulators," *Journal of Guidance, Control, and Dynamics*, Vol. 12, No. 5, 1989, pp. 659–671.

[2]Singh, R. P., VanderVoort, R. J., and Likins, P. W., "Dynamics of Flexible Bodies in Tree Topology—A Computer-Oriented Approach," *Journal of Guidance, Control, and Dynamics*, Vol. 8, No. 5, 1985, pp. 584–590.

[3]Bodley, C., Devers, A., Park, A., and Frisch, H., "A Digital Computer Program for Dynamic Interaction and Simulation of Controls and Structures (DISCOS)," NASA TP 1219, May 1978.

[4]Kwak, M. K., and Meirovitch, L., "New Approach to the Maneuvering and Control of Flexible Multibody Systems," *Journal of Guidance, Control, and Dynamics*, Vol. 15, No. 6, 1992, pp. 1342–1353.

[5]Book, W. J., "Recursive Lagrangian Dynamics of Flexible Manipulator Arms Via Transformation Matrices," *International Journal of Robotics Research*, Vol. 3, No. 3, 1984, pp. 87–101.

[6]Banerjee, A. K., and Lemak, M. E., "Multi-Flexible Body Dynamics Capturing Motion-Induced Stiffness," *Journal of Applied Mechanics*, Vol. 58, Sept. 1991, pp. 766–775.

[7]Anon., "GRASP Theory Manual," Grumman, Space Station Integration Division, 1991.

[8]Hughes, P. C., "Modal Identities for Elastic Bodies, with Application to Vehicle Dynamics and Control," *Journal of Applied Mechanics*, Vol. 47, March 1980, pp. 177–184.

[9]Hwang, Y. L., and Shabana, A. A., "Dynamics of Flexible Multibody Space Cranes Using Recursive Projection Methods," *Computers and Structures*, Vol. 43, No. 3, 1992, pp. 549–563.

[10]Cannon, R. H., Jr., and Schmitz, E., "Initial Experiments on the End-Point Control of a Single-Link Flexible Arm," *International Journal of Robotics Research*, Vol. 3, No. 3, 1984, pp. 62–75.

[11]Hecht, N. K., and Junkins, J. L., "Near-Minimum-Time Control of a Flexible Manipulator," *Journal of Guidance, Control, and Dynamics*, Vol. 15, No. 2, 1992, pp. 77–481.

[12]Oakley, C. M., and Cannon, R. H., Jr., "Theory and Experiments in Selecting Mode Shapes for Two-Link Flexible Manipulators," *Proceedings of the First International Symposium in Experimental Robotics I: the First International Symposium* (Montreal), edited by V. Hayward and O. Khatib, Springer–Verlag, Berlin, New York, 1989.

[13]Canavin, J. R., and Likins, P. W., "Floating Reference Frames for Flexible Spacecraft," *Journal of Spacecraft and Rockets*, Vol. 14, No. 12, 1977, pp. 724–732.

[14]Padilla, C. E., and von Flotow, A. H., "Non-Linear Strain-Displacement Relations in Flexible Multibody Dynamics," *Journal of Guidance, Control, and Dynamics*, Vol. 15, No. 1, 1992, pp. 128–136.

[15]Tadikonda, S. S. K., and Baruh, H., "Gibbs Phenomenon in Structural Mechanics," *AIAA Journal*, Vol. 29, No. 10, 1991, pp. 1488–1497.

[16]Meirovitch, L., *Computational Methods in Structural Dynamics*, Sijthoff and Noordhoff, Alphen aan den Rijn, The Netherlands, 1980.

[17]Tadikonda, S. S. K., and Chang, H. T., "On The Geometric Stiffness Matrices in Flexible Multibody Dynamics," *Dynamics of Flexible Multibody Systems: Theory and Experiment*, DSC-Vol. 37, American Society of Mechanical Engineers, New York, 1992, pp. 223–230; also *Journal of Vibration and Acoustics* (to be published).

[18]Kane, T. R., Ryan, R. R., and Banerjee, A. K., "Dynamics of a Cantilever Beam Attached to a Moving Base," *Journal of Guidance, Control, and Dynamics*, Vol. 10, No. 4, 1987, pp. 139–151.

[19]Ryan, R. R., "Flexibility Modeling Methods in Multibody Systems," Ph.D. Thesis, Mechanical Engineering, Stanford Univ., Stanford, CA, 1986.

[20]Hanagud, S., and Sarkar, S., "Problem of the Dynamics of a Cantilever Beam Attached to a Moving Base," *Journal of Guidance, Control, and Dynamics*, Vol. 12, No. 3, 1989, pp. 438–441.

[21]Simo, J. C., and VuQuoc, L., "The Role of Nonlinear Theories in Transient Dynamic Analysis of Flexible Structures," *Journal of Sound and Vibration*, Vol. 119, No. 3, 1987, pp. 487–508.

[22]Meirovitch, L., and Kwak, M. K., "Rayleigh–Ritz Based Substructure Synthesis for Flexible Multibody Systems," *AIAA Journal*, Vol. 29, No. 10, 1991, pp. 1709–1719.